Shock and vibration response of museum objects during transportation

Shock and vibration response of museum objects during transportation

Thomas W J Hutchin[1,2,3], **Timothy P Waters**[1], **and Verena Kotonski**[2]

[1] University of Southampton, University Road, Southampton SO17 1BJ, United Kingdom
[2]The British Museum, Great Russell Street, London, WC1B 3DG, United Kingdom
[3]Author to whom any correspondence should be addressed.

Email: thomas.hutchin@soton.ac.uk

Keywords: Shock response spectrum, vibration, transport, damage, museum

Abstract. Museum objects are frequently transported by road and air when toured internationally or when moved between storage facilities which exposes them to a range of vibration and shock inputs. Many of these vulnerable objects have incipient damage such as cracks, loose joints, partial delamination or failing repairs which can be exacerbated in transit. It is the conservator's responsibility to select which objects are safe to travel, largely based on experience and professional judgement. A joint research programme between the University of Southampton and the British Museum aims to develop a scientific framework to aid and inform such judgements. A central research question, and the focus of this paper, is which methods of transport are potentially most damaging?

Vibration measurements were acquired during transit by car, train, ferry and commercial airliner. A moving average kurtosis is used to identify near-Gaussian and non-Gaussian segments in a time signal. Acceleration shock response spectra (SRS) are presented for a number of impulsive events, and corresponding vibration response spectra (VRS) shown for more normally distributed random inputs. Laboratory based vibration testing was carried out on a museum artefact packed in bespoke foam packaging inside a standard wooden transport crate. The modal response, combined with SRS and VRS, enabled the response of the object and the suitability of the packaging in reducing the response to different real-life stimuli to be assessed. Actual measurements on the artefact in transit also enabled the accuracy of SRS and VRS in predicting peak and RMS acceleration levels to be quantified.

1 Introduction

Museums regularly need to transport objects: from stores to laboratories, workshops and galleries, or to national and international loan venues. The various reasons for travel also introduce a range of transport types including road, train, ferry, and air freight. Museum objects are often vulnerable to shock and vibration arising from transportation due to incipient damage such as cracks, delamination, or material degradation. Museums must therefore make informed decisions as to which items are safe to travel and how best to mitigate the risks posed, e.g. by choice of transport or packing methods. Such judgements are often made by heritage specialists without recourse to engineering tools or knowledge of vibration. The ultimate aim of this collaborative project with the British Museum is to provide

guidance and simple tools to aid the decision-making process.

There has been significant prior work on the effects of shock and vibration on historic buildings, due to either seismic activity or nearby construction work, e.g. [1,2]. However, there have been surprisingly few previous studies on the effects of shock and vibration on portable artefacts. Some relate to 2D objects such as paintings [3,4], which are more uniform in construction and geometry. Marcon [5] studied the vibration environment of various transport methods using empirical data, and discussed the probable causes of vibration for each transport type. The authors expected that road methods will have the highest severity of vibration, followed by rail, ships and air from the data presented in the paper. It is also noted that handling operations at transfer points will be a major hazard. The data used in this study is not specific to the transport of paintings, so can be applied to other types of object. Fewer papers have investigated 3D objects, which are far more varied. One notable study on 3D museum objects by Thickett [6] reported the vibration levels at which damage was observed when construction work was taking place, and gave detailed descriptions of how to measure and monitor damage to objects. Kamba et al. [7] monitored vibration in packing crates for 3D objects during several journeys. Time signals are presented for several journeys and power spectral densities reported specifically for skate trolley movements at airports. The authors conclude that movements by skate trolley subject objects to the highest levels of vibration, followed by road and air. More recently, Kotonski et al. presented a field trial of a crate-within-a-crate design solution featuring wire rope isolators to reduce the transmission of vibration to fragile contents [8]. The authors also developed a calculator tool to select isolators for various objects.

Beyond the heritage sector, a commonly used method for assessing the resilience of objects exposed to shock is the Shock Response Spectrum (SRS). The method computes the peak response of a single degree-of-freedom system to an input of concern and quantifies the sensitivity of the response to changes in natural frequency and damping. Since it was first proposed by Biot [9] in 1932 it has found many applications in fields such as earthquakes, explosions and road speed bumps [10–12]. For example, Goyal et al. [13] discussed usage of the SRS to design shock protection for portable electronic products and compared its effectiveness with a damage boundary approach, another method of vibration prediction. The authors concluded that, while the SRS approach has its limitations, it is useful in determining the effects of shock duration on the system response. The SRS concept has been extended to multiple degree of freedom systems [14] but it is not widely used.

Analogous to the SRS is the vibration response spectrum (VRS) which, to the authors' knowledge, was first proposed by Irvine [15] some 70 years later and has been used, for example, to aid the design of military airborne equipment [16]. By producing a VRS for various phases of flight, the expected RMS acceleration limits can be predicted for a range of systems with varying natural frequencies. The VRS can be used for acceptance testing where the equipment's natural frequency is known. The VRS has also been used in the design of a floor structure to minimise annoyance due to occupants' footfall in an apartment [17].

Other types of response spectra, i.e. where natural frequency is the independent variable, have been proposed in the literature for specific purposes. The kurtosis response spectrum quantifies how the kurtosis of the response to a given input vibration varies with natural frequency [18]. A large value is indicative of a higher likelihood of extreme events during transportation. The authors applied this to aid the design of antivibration packaging. Another variant of response spectra is the fatigue damage spectrum which combines the SRS with S-N curves to predict the fatigue of an object [19].

In this study, vibration measurements have been acquired for a range of modes of transport. In practice, there may be little or no prior knowledge of the dynamic response of museum objects due to lack of opportunity to conduct vibration tests combined with the complexities of generating finite element models of intrinsically damaged objects of unknown material properties. The standard shock response spectrum and vibration response spectrum are used here as simple means of predicting the acceleration experienced by an object from prior knowledge of only its fundamental natural frequency and modal damping. This investigation takes as its case study a nominally rigid test object for which the fundamental mounting resonance arises from its suspension within foam packaging. The SRS and VRS are potentially useful in two respects: first, quantifying the sensitivity of the response with respect to natural frequency from which foam materials and thicknesses can be selected, and second,

in evaluating the relative harshness of different modes of transport.

The paper is organised as follows. Section 2 provides a brief overview of the well-known SRS and analogous but less familiar VRS. A higher order statistic – kurtosis - is also recalled as a means to discriminating between normally distributed random vibration and inputs with extreme, transient events. Section 3 outlines the experimental methodology adopted. Section 4 presents and discusses the SRS and VRS for different modes of transport and compares their predictions with actual measurements on the test object. Conclusions are drawn and future work are discussed in Section 5.

2 Theory

2.1 Higher Order Statistics

Lower order statistics are averages of a random variable raised to the power one (mean) or two (variance). Kurtosis is the most commonly used higher order statistic in which the variable is raised to the power four, and is thus defined as

$$k = \frac{\frac{1}{n}\sum_{i=1}^{n}(x_i - \bar{x})^4}{\left(\sqrt{\frac{1}{n}\sum_{i=1}^{n}(x_i - \bar{x})^2}\right)^2} \tag{1}$$

The kurtosis of a normally distributed random variable is three. When applied to time signals, a kurtosis value much greater than three is indicative of the presence of impulsive events. Kurtosis can be evaluated on the basis of a short-time moving average through the signal to identify which parts are more impulsive and which parts are more random [20].

2.2 Shock Response Spectra

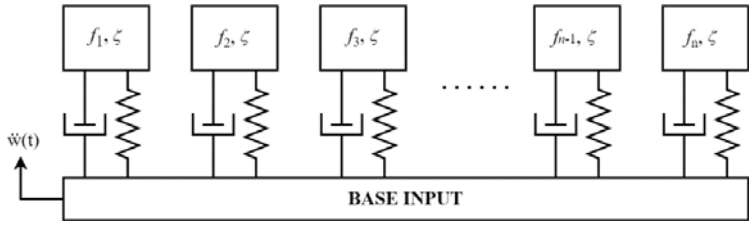

Figure 1. Diagram demonstrating different SDOF systems with a common base input.

An individual resonance of a dynamic system can often be represented by a single degree-of-freedom (SDOF) with appropriately chosen natural frequency (f) and damping ratio (ζ). One can consider many such systems of different natural frequency f_1 to f_n, as shown in Fig. 1, subjected to the same base input. The equation of motion for a SDOF system of natural frequency f_n to a displacement input at the base $w(t)$ is given by [14]

$$-\ddot{w}(t) = \ddot{z}(t) + 2\zeta\omega_n\dot{z}(t) + \omega_n^2 z(t) \tag{2}$$

where $\omega_n = 2\pi f_n$ is the circular natural frequency. The time response of each system can be readily computed for arbitrary inputs using one of many Runge-Kutta based numerical solvers such as ODE45 in MATLAB. The shock response spectrum (SRS) is a plot of the peak response as a function of natural frequency, usually for a fixed damping ratio. The peak of maximum amplitude is chosen, i.e. in the positive or negative direction, which is often referred to as the maximax response. The SRS is used extensively to infer ranges of natural frequencies that are most likely to give rise to damage for a given input, or to compare the severity of different inputs e.g. [21].

2.3 Vibration Response Spectra

Vibration Response Spectra (VRS) are defined in an analogous way to the SRS except that the root-

mean-square (RMS) instead of the peak magnitude is plotted against natural frequency [14]. The same time responses computed for the SRS can be reprocessed thereby necessitating negligible additional computational effort. Alternatively, the RMS of the response can be obtained in the frequency domain as follows [15]

$$\ddot{z}_{RMS}(f_n,\zeta) = \sqrt{\sum_{i=1}^{N} \frac{1+(2\zeta\rho_i)^2}{(1-\rho_1^2)^2+(2\zeta\rho_i)^2} S_{\ddot{w}\ddot{w}}(f_i)\Delta f}\,, \qquad \rho_i = f_i/f_n \tag{3}$$

where $\rho_i = f_i/f_n$ is the ratio of excitation frequency to natural frequency, Δf is the frequency resolution, and $S_{\ddot{w}\ddot{w}}$ is the power spectral density (PSD) of the acceleration input, which can be readily computed using Welch's method [22].

3 Testing Methodology

3.1 Test Object

The object chosen for this study was a wooden stool, shown in Fig. 2, of unknown origin and age which is part of the British Museum's handling/training collection. It is approximately 0.4 m in diameter and has a mass of 1.5 kg. The object was packed in polyurethane foam cut to form inside a wooden crate by specialists at the museum.

3.2 Hammer Testing

An instrumented impact hammer test was performed on the test object whilst packaged inside the crate to identify the natural frequencies and damping ratios of the assembly. The crate's lid was removed and small cut-outs made in the Tyvek (lining material) to allow for access by the accelerometer (PCB 353B32) and hammer (PCB 086C03). The acceleration and impact force signals were acquired and frequency response functions (FRF) of acceleration with respect to force obtained by a DataPhysics Quattro data acquisition system. The fundamental natural frequency and damping ratio were estimated using the circle fitting method [23].

Figure 2. Photographs of (a) the unpackaged test object, (b) the packaged test object with the crate lid removed, (c) the internal packaging and (d) the crate in the luggage compartment of the test vehicle. Vibration loggers highlighted in (b) and (d).

3.3 Vibration In Transportation

Environmental vibration measurements were captured in two separate experimental campaigns. In the first, a vibration data logger was fixed to the base rail of a passenger seat on return flights from London Stansted to Malaga by an aircraft maintenance engineer. The outbound flight was turbulent throughout, and the return flight was not. The flights were of comparable single aisle jet aircraft from different manufacturers. The second journey was a return trip from Essex in the south-east of England to Calais, France incorporating road, ferry, and train (Eurotunnel). In this test, the crate containing the test object was transported enabling measurement of both the vibration exposure of the crate and the test object inside. The crate remained in the luggage compartment of the car, a Volvo XC70, throughout the journey. Loading and unloading of the car onto the ferry and train were intentionally included in the measurements to capture any related shocks. In both tests MSR165 data loggers were used which were set to 14-bit resolution, a range of ±15 g and a sampling rate of 1600 Hz giving an operational frequency range of 0-800 Hz. Figures 2(b) and (d) show the placement of the two loggers on the crate and the test object. The logger on the crate was attached using three screws whereas the external sensor of the logger on the object was attached using double sided cloth adhesive tape.

4 Results

4.1 Modal Analysis of Test Object

Figure 3 shows the magnitude of the accelerance FRF of the packaged test object. The fundamental natural frequency occurs at 38.8 Hz and the damping ratio is 0.24. This frequency is much lower than the first elastic mode of the stool when suspended on bungees so is assumed to be a rigid body mode of the test object vibrating against the stiffness of the foam. Other prominent but highly damped modes occur at about 85 Hz and 235 Hz.

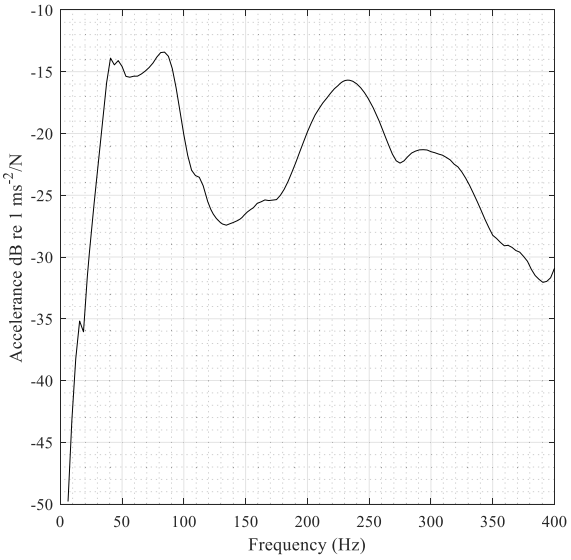

Figure 3. Magnitude of the accelerance FRF of the packaged test object.

4.2 Moving average kurtosis

Moving average kurtosis graphs were produced from the recordings of each transport type from which periods of transient activity could be identified. For brevity only one example is presented which is for vibration in the vertical direction on the non-turbulent flight, see Fig. 4(a). The time signal was separated into 740 overlapping segments giving a time resolution of about 13 seconds. Figure 4(b) shows the raw time signal. When the aircraft is in cruise - between 0.5 hours and 2 hours - the kurtosis

is close to three indicating that the random vibration is normally distributed. Jet noise and turbulence are the most likely predominant sources. In contrast, periods between 0 – 0.5 hours and beyond 2 hours are more impulsive due to take-off and landing, as evidenced by kurtosis values much larger than three.

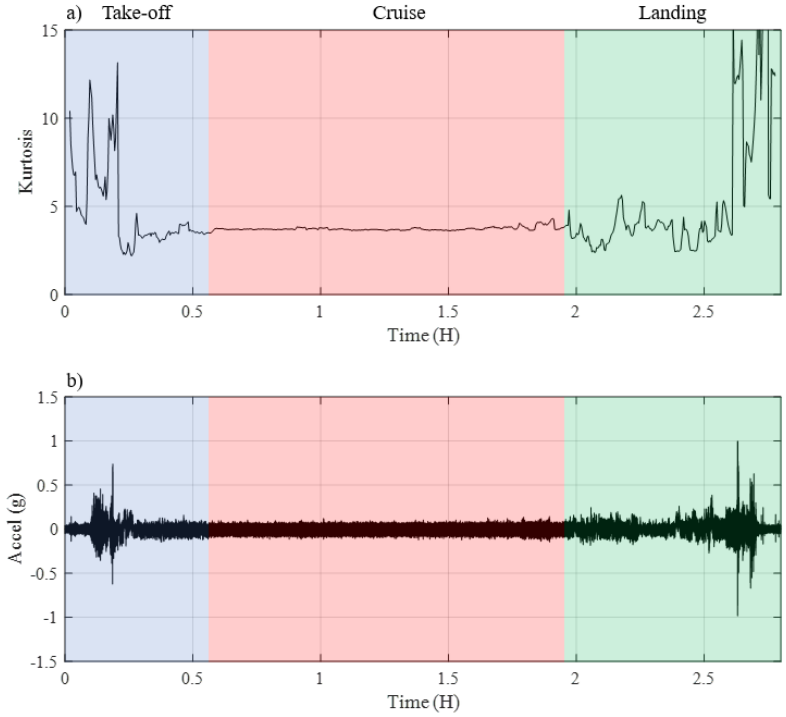

Figure 4. (a) Moving average kurtosis and (b) time signal of non-turbulent flight.

4.3 Shock Response Spectra

SRS were computed for a damping ratio of $\zeta = 0.24$, corresponding to that measured for the fundamental mounting resonance of the test object in its packaging, and for a natural frequency range from 1 Hz to 800 Hz as dictated by the sampling rate of the vibration measurements. Fig. 5(a) overlays the SRS for the outbound (turbulent) and inbound (non-turbulent) flights. Below 30 Hz, the SRS predicts that the two flights result in similar peak acceleration levels, whereas the peak acceleration is higher for the turbulent flight above 30 Hz. The graph suggests that a fundamental mode of the object within its packaging of about 38 Hz would have given rise to peak acceleration levels of over 1.9 g for the turbulent flight, and above 1.5g for the non-turbulent flight. Lowering the mounting resonance will increase the performance for both flights but would require softer foam undergoing a higher static deflection due to the object's weight.

Fig. 5(b) overlays the SRS for all three modes of transport in the trip to France, for which the crate was transported and instrumented. All curves exhibit a peak at about 10-20 Hz which was identified through instrumented hammer testing as attributable to resonances of the crate. All three legs of the journey are predicted to cause similar amplitudes of shock over the full range of natural frequencies. This is possibly because similar shocks occurred during loading and unloading of the vehicle onto the train and ferry and the vehicle travelling over discontinuities in the road surface.

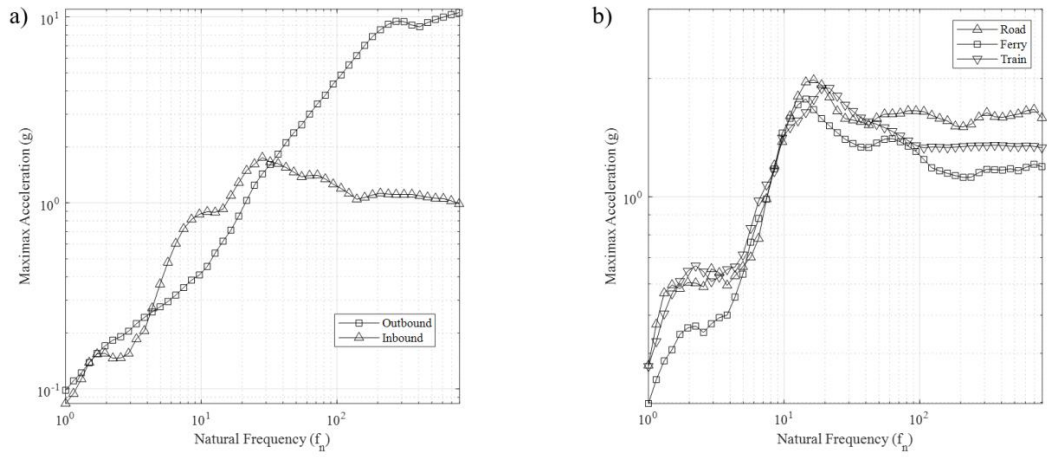

Figure 5. (a) The SRS of two flights and (b) for three modes of transport, $\zeta = 0.24$.

4.4 Vibration Response Spectra

VRS were produced for the two flight recordings and the three transport types used during the return trip from England to France. The same natural frequency range and damping ratio were chosen as for the SRS.

Figure 6(a) shows the VRS of the two flights. The turbulent outbound flight, much like the SRS of the same flight, contained more high-frequency vibration, causing a significant increase in predicted response for systems with a natural frequency above 60 Hz. This is closer to the frequency spectrum proposed by Marcon [5] for air freight, compared to the non-turbulent flight. The peak response is much less sensitive to natural frequency for the inbound flight.

Figure 6(b) shows the VRS for the three transport types of the return trip to France. The RMS acceleration for the car journey is about three to four times higher than for the ferry and train. All three curves show a peak at 10-20 Hz due to crate resonances. The small peak at 2 Hz is possibly attributable to the bounce mode of the vehicle on its suspension. Again, a mounting resonance of the packaged object of below 10 Hz is recommended which is consistent with complementary work commissioned by the British Museum [8].

4.5 Comparing Predicted and Measured Shock and Vibration

The SRS and VRS are potentially useful tools to predict, qualitatively at least, the peak and RMS response of any system that can be approximately represented by a simple SDOF system. This is now illustrated for the trip to France for which acceleration measurements were available on both the crate and the test object itself. Implicit in the assumed SDOF model used in both the SRS and VRS is that motions of the crate and the test object can be considered uniaxial. In practice, rigid body rotation or elastic deformation of either would violate this assumption.

Table 1 compares the peak accelerations predicted by the SRS calculated in section 4.3 with their measured counterparts on the test object. The SRS model under-predicts the peak acceleration of the road transport but over-predicts the rail and ferry transport.

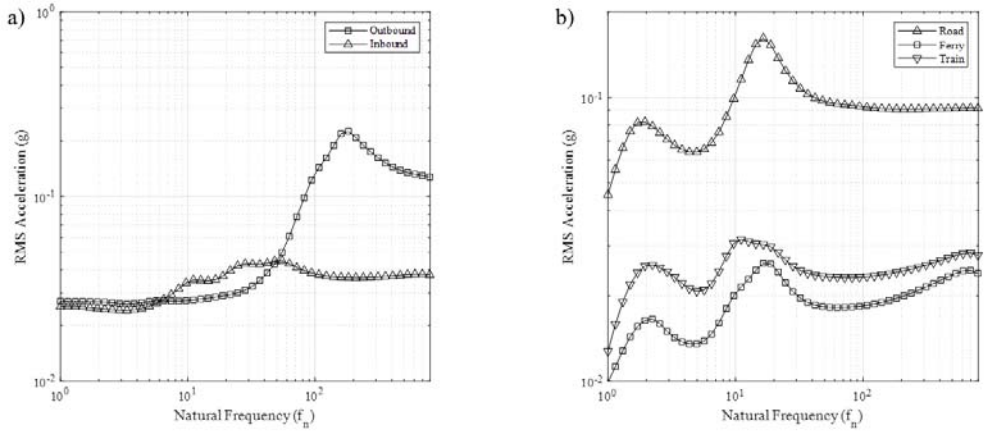

Figure 6. (a) The VRS of two flights and (b) VRS of three modes of transport, $\zeta = 0.24$.

Type of Transport	Predicted Maximax Acceleration (g)	Measured Maximax Acceleration (g)	Percentage Difference
Road	1.54	1.83	-15.5%
Ferry	1.33	1.21	+9.5%
Train	1.57	1.45	+8.2%

Table 1. Predicted and measured maximax accelerations for three transport types.

Type of Transport	Predicted RMS Acceleration (g)	Measured RMS Acceleration (g)	Percentage Difference
Road	0.101	0.109	-7.0%
Ferry	0.019	0.022	-16.7%
Train	0.024	0.026	-8.1%

Table 2. Predicted and measured RMS accelerations for three transport types.

Table 2 compares the RMS acceleration values predicted by the VRS with the measured values on the test object. The VRS model is reasonably accurate and correctly rank orders the three modes of transport. Given some commonality in the assumptions underpinning the SRS and VRS it is clear why the two models have a similar accuracy in this case study. It should be noted, however, that the actual response is likely to be multi-modal given high modal damping which violates the fundamental assumption of both the SRS and VRS.

5 Conclusions

Vibration measurements have been collected for four modes of transport: air, car, train, and sea ferry. Shock Response Spectra (SRS) and Vibration Response Spectra (VRS) have been computed for each to predict and compare the peak and RMS vibration levels that a supposedly rigid object would be exposed to when packaged in foam inside a transportation crate. The chosen test object was a wooden stool from the British Museum's handling collection. In all modes of transport, it is predicted that peak and RMS acceleration levels can be substantially reduced if mounting resonances of the object within its packaging of less than about 10 Hz can be achieved. Acceleration measurements on the test object itself were compared with predicted values from the SRS and VRS. The VRS captured the RMS vibration levels reasonably accurately; maximax predictions from the SRS were also reasonably accurate. The SDOF modelling assumptions are unlikely to be met in this case given the high damping

of the mounting resonances. Both spectra proved useful in identifying a target maximum natural frequency for the object in its packaging. Future work aims to develop empirical models to predict the response of resonant objects in packaging from limited vibration measurements on museum objects.

Acknowledgements

This work was supported by the Arts and Humanities Research Council in the UK (Grant Ref - AH/W002183/1). The authors would like to thank Emma Gillam (British Museum, Department of Collection Care) for creating the bespoke packaging used, and Phillip Hutchin for his assistance in acquiring the transport vibration data.

References

[1] Saisi A, Gentile C, Guidobaldi M, Cantini L. *Dynamic and Seismic Assessment of the Gabbia Tower in Mantua, Italy*. In: Research for Development. 2015. p. 141–53.
[2] Johnson AP, Robert Hannen W, Zuccari F. *Vibration control during museum construction projects*. J Am Inst Conserv. 2013;**52**(1):30–47.
[3] Saunders D. *Monitoring shock and vibration during the transportation of paintings*. Natl Gall Tech Bull. 1998;**19**:64–73.
[4] Läuchli M, Bäschlin N, Hoess A, Fankhauser T, Palmbach C, Ryser M. *Packing systems for paintings: Damping capacity in relation to transport-induced shock and vibration*. In: Presentation at ICOM-CC 17th Triennial Conference, Melbourne. 2014. p. 19.
[5] Marcon PJ. *Shock, vibration, and the shipping environment*. In: Marcon PJ, editor. Art in Transit: Studies in the Transport of Paintings. Washington, DC, USA: National Gallery of Art; 1991. p. 121–32.
[6] Thickett D. *Vibration damage levels for museum objects*. In: ICOM Committee for Conservation 13th Triennial Meeting Rio de Janeiro. 2002.
[7] Kamba N, Wada H, Tsukada M, Takagi Y, Imakita K. *Measurement and Analysis of the Global Transport Environment for Packing Cases for Artifacts*. Stud Conserv. 2008;**53**(sup1):60–3.
[8] Kotonski V, Kracht K, York E, Barton C. *Protecting Three-Dimensional Museum Collections During Transport: Engineering and Evaluation of Transport Crates Featuring Wire-Rope Isolators for Improved Vibration Mitigation*. Stud Conserv. 2022;1–10.
[9] Biot MA. *Transient oscillations in elastic systems*. California Institute of Technology; 1932.
[10] Choi M. *Experimental prediction of shock response spectra of point-wise explosive pyroshock in a space launcher composite structure using laser pulse excitation and in-line filtering*. SAE Int J Aerosp. 2013;**6**(1):65.
[11] Hacıefendioğlu K, Banerjee S, Soyluk K, Köksal O. *Multi-point response spectrum analysis of a historical bridge to blast ground motion*. Struct Eng Mech. 2015;**53**(5):897–919.
[12] Waters TP, Hyun Y, Brennan MJ. *The Effect of Dual-Rate Suspension Damping on Vehicle Response to Transient Road Inputs*. J Vib Acoust. 2009 Jan 5;**131**(1).
[13] Goyal S, Papadopoulos JM, Sullivan PA. *Shock Protection of Portable Electronic Products: Shock Response Spectrum, Damage Boundary Approach, and Beyond*. Shock Vib. 1997;**4**:169–91.
[14] Sisemore C, Babuška V. *Multi-Degree-of-Freedom Systems*. In: The Science and Engineering of Mechanical Shock. Springer; 2020. p. 199–227.
[15] Irvine T. *An Introduction to the Vibration Response Spectrum* [Internet]. Vibrationdata. 2009 [cited 2022 Dec 12]. p. 1–20. Available from: http://www.vibrationdata.com/tutorials2/vrs.pdf
[16] Das BK, Kumar P. *Tailoring of specifications for random vibration testing of military airborne equipments from measurement*. Int J Res Eng Technol. 2015;**4**(12):293–9.
[17] Chen J, Xu R, Zhang M. *Acceleration response spectrum for predicting floor vibration due to occupant walking*. J Sound Vib. 2014;**333**(15):3564–79.
[18] Hosoyama A, Tsuda K, Horiguchi S. *Development and validation of kurtosis response spectrum analysis for antivibration packaging design taking into consideration kurtosis*.

Packag Technol Sci. 2020;**33**(2):51–64.
[19] McNeill SI. *Implementing the fatigue damage spectrum and fatigue damage equivalent vibration testing*. In: Presented at the 79th Shock and Vibration Symposium: October. 2008. p. 30.
[20] Hinton PR. *Statistics explained*. Third edit. London: Routledge, Taylor & Francis Group; 2014.
[21] Olofsson U, Svensson T, Torstensson H. *Response spectrum methods in tank-vehicle design*. Exp Mech. 1995;**35**(4):345–51.
[22] Brandt A. *Noise and Vibration Analysis: Signal Analysis and Experimental Procedures* [Internet]. Wiley; 2011. (EBL-Schweitzer).
[23] Ewins DJ. *Modal Testing: Theory, Practice and Application*. Wiley; 2009. (Mechanical Engineering Research Studies: Engineering Dynamics Series).